Cancer Research

Targeting HER2-Positive Breast Cancer with Trastuzumab-DM1, an Antibody–Cytotoxic Drug Conjugate

Gail D. Lewis Phillips, Guangmin Li, Debra L. Dugger, et al.

Cancer Res 2008;68:9280-9290.

Targeting HER2-Positive Breast Cancer with Trastuzumab-DM1, an Antibody–Cytotoxic Drug Conjugate

Gail D. Lewis Phillips,[1] Guangmin Li,[1] Debra L. Dugger,[1] Lisa M. Crocker,[1] Kathryn L. Parsons,[1] Elaine Mai,[1] Walter A. Blättler,[2] John M. Lambert,[2] Ravi V.J. Chari,[2] Robert J. Lutz,[2] Wai Lee T. Wong,[1] Frederic S. Jacobson,[1] Hartmut Koeppen,[1] Ralph H. Schwall,[1] Sara R. Kenkare-Mitra,[1] Susan D. Spencer,[1] and Mark X. Sliwkowski[1]

[1]Genentech, Inc., South San Francisco, California and [2]ImmunoGen, Inc., Waltham, Massachusetts

Abstract

HER2 is a validated target in breast cancer therapy. Two drugs are currently approved for HER2-positive breast cancer: trastuzumab (Herceptin), introduced in 1998, and lapatinib (Tykerb), in 2007. Despite these advances, some patients progress through therapy and succumb to their disease. A variation on antibody-targeted therapy is utilization of antibodies to deliver cytotoxic agents specifically to antigen-expressing tumors. We determined *in vitro* and *in vivo* efficacy, pharmacokinetics, and toxicity of trastuzumab-maytansinoid (microtubule-depolymerizing agents) conjugates using disulfide and thioether linkers. Antiproliferative effects of trastuzumab-maytansinoid conjugates were evaluated on cultured normal and tumor cells. *In vivo* activity was determined in mouse breast cancer models, and toxicity was assessed in rats as measured by body weight loss. Surprisingly, trastuzumab linked to DM1 through a nonreducible thioether linkage (SMCC), displayed superior activity compared with unconjugated trastuzumab or trastuzumab linked to other maytansinoids through disulfide linkers. Serum concentrations of trastuzumab-MCC-DM1 remained elevated compared with other conjugates, and toxicity in rats was negligible compared with free DM1 or trastuzumab linked to DM1 through a reducible linker. Potent activity was observed on all HER2-overexpressing tumor cells, whereas nontransformed cells and tumor cell lines with normal HER2 expression were unaffected. In addition, trastuzumab-DM1 was active on HER2-overexpressing, trastuzumab-refractory tumors. In summary, trastuzumab-DM1 shows greater activity compared with nonconjugated trastuzumab while maintaining selectivity for HER2-overexpressing tumor cells. Because trastuzumab linked to DM1 through a nonreducible linker offers improved efficacy and pharmacokinetics and reduced toxicity over the reducible disulfide linkers evaluated, trastuzumab-MCC-DM1 was selected for clinical development. [Cancer Res 2008;68(22):9280–90]

Introduction

The HER2 (ErbB2) receptor tyrosine kinase is a member of the epidermal growth factor receptor family of transmembrane receptors. These receptors, which also include HER3 (ErbB3) and HER4 (ErbB4), are known to play critical roles in both development and cancer (1, 2). Importantly, amplification and overexpression of HER2 occur in 20% to 25% of human breast cancer and are predictive of poor clinical outcome (3, 4). Because of the role of HER2 in breast cancer pathogenesis and the accessibility of the extracellular portion of the receptor, HER2 was recognized as a potential candidate for targeted antibody therapy. The humanized HER2 antibody, trastuzumab (Herceptin), was approved by the Food and Drug Administration in 1998 for use in metastatic breast cancer and has subsequently shown clinical benefit when used, in combination with cytotoxic chemotherapy, as first-line or adjuvant therapy (5, 6). Importantly, trastuzumab improves overall survival in early breast cancer after chemotherapy compared with observation alone (6). Increased survival after only 2 years of follow-up is impressive in breast cancer. Tamoxifen is the only other breast cancer treatment that is reported to offer a survival benefit in this short-time period (6).

Although the mechanisms for response to trastuzumab are not completely understood, clinical benefit is attributed to interference with signal transduction pathways, impairment of extracellular domain (ECD) cleavage, inhibition of DNA repair, decreased angiogenesis; as well as induction of cell cycle arrest, and antibody-mediated cellnlar cytotoxicity (7, 8). Despite these diverse mechanisms of action, a significant proportion of patients treated with trastuzumab either do not respond initially or relapse after experiencing a period of clinical response (5, 9). Progression through trastuzumab-containing therapy is attributed to aberrant activation of signaling pathways, such as the phosphatidylinositol 3-kinase pathway (10–12), activation of compensatory signaling either through up-regulation of the insnlin-like growth factor-I receptor (13, 14) or ErbB/HER ligands (15, 16) or generation of a constitutively active truncated form of HER2, designated p95HER2 (17, 18).

Direct covalent coupling of cytotoxic agents to monoclonal antibodies is an alternative to naked antibody-targeted therapy. To date, antitumor antibodies have been linked to cytotoxic agents, such as the calicheamicins, auristatins, maytansinoids and derivatives of CC1065 (19–22). Currently, only one such conjugate, anti-CD33 conjugated to calicheamicin (gemtuzumab ozogamicin or Mylotarg), has been granted marketing approval for the treatment of relapsed acute myeloid leukemia (23).

Maytansinoids are derivatives of the antimitotic drug maytansine. These agents bind directly to microtubules in a manner similar to the *Vinca* alkaloids (24, 25). Antibody-maytansinoid conjugates directed toward cancer antigens, such as CanAg (cantuzumab mertansine and IMGN242), prostate-specific membrane antigen (MLN2704), CD56 (IMGN901), CD33 (AVE9633), and

Note: Current address for H. Koeppen: M. D. Anderson Cancer Center, Houston, TX 77030.

Requests for reprints: Gail D. Lewis Phillips, Genentech, Inc., 1 DNA Way, South San Francisco, CA 94080. Phone: 650-225-2201; Fax: 650-225-1411; E-mail: gdl@gene.com or Mark X. Sliwkowski, Genentech, Inc., 1 DNA Way, South San Francisco, CA 94080. Phone: 650-225-1247; Fax: 650-225-5770; E-mail: marks@gene.com.

doi:10.1158/0008-5472.CAN-08-1776

CD44v6 (bivatuzumab mertansine) are in early stages of clinical testing (20, 26–28). Because HER2 is highly differentially expressed on breast tumor cells (1–2 million copies per cell) compared with normal epithelial cells, HER2 represents an ideal target for antibody-drug conjugate (ADC) therapy. Numerous preclinical and clinical studies indicate that trastuzumab combines extremely well with microtubule-directed agents (29–32). Given the mechanism of action and potency of maytansine, it was deemed to be a particularly attractive cytotoxic agent to conjugate to trastuzumab. Herein, we describe the efficacy, pharmacokinetic properties, and safety of several trastuzumab-maytansinoid conjugates, with particular emphasis on the chemical nature of the linker.

Materials and Methods

Cell lines and reagents. Tumor cell lines (breast carcinoma BT-474, SK-BR-3, MCF7, MDA-MB-468, MDA-MB-361, HCC1954, lung carcinoma Calu 3, and ovarian carcinoma line SK-OV-3) and MCF 10A breast epithelial cells were obtained from American Type Culture Collection. The breast tumor line KPL-4 was obtained from Dr. J. Kurebayashi (33), and MKN7 gastric carcinoma cells were from Mitsubishi Corp. Cells were maintained in Ham's F-12: high glucose DMEM (50:50) supplemented with 10% heat-inactivated fetal bovine serum and 2 mmol/L L-glutamine (all from Invitrogen Corp.). Normal human cell lines [human mammary epithelial cells (HMEC) and normal human epidermal keratinocytes (NHEK)] and the corresponding culture medium (MEGM and KGM, respectively) were obtained from Cambrex. The BT474-EEI cell line was derived by subculturing BT-474 tumors grown *in vivo* in the absence of estrogen pellet supplementation (exogenous estrogen independent) and is resistant both *in vitro* and *in vivo* to trastuzumab treatment.

Active agents used for cell culture and animal studies were the antibody trastuzumab (Genentech, Inc.), trastuzumab-maytansinoid ADC (ImmunoGen, Inc.), and the control ADC, anti–IL-8-MCC-DM1. The maytansinoid, DM1, was conjugated to trastuzumab through SPP, SMCC, or SPDP linkers (Fig. 1; refs. 24, 34); the thiol-containing maytansinoids, DM3 and DM4, which have methyl groups adjacent to their sulfhydryl group were linked to trastuzumab with the SSNPP linker (ImmunoGen, Inc.). All trastuzumab ADCs had an average molar ratio of 3 to 3.6 maytausinoid molecules per antibody. The drug-antibody molar ratio for trastuzumab-MCC-DM1 and trastuzumab-SPP-DM1 was 3.2 for cell culture and xenograft studies, 3.6 for trastuzumab-SPP-DM1 used in the rat toxicity study, and 3.8 for anti–IL-8-MCC-DM1.

Cell viability and cell death assays. The effects of trastuzumab and trastuzumab-maytansinoid conjugates on tumor cell viability were assessed using Cell Titer-Glo (Promega Corp.). Cells were plated in black-walled 96-well plates (20,000 per well for BT-474; 10,000 cells per well for all other lines) and allowed to adhere overnight at 37°C in a humidified atmosphere of 5% CO_2. Medium was then removed and replaced by fresh culture medium containing different concentratious of trastuzumab, trastuzumab ADC, or free DM1, and the cells incubated for varying periods of time. After each time point, Cell Titer-Glo reagent was added to the wells for 10 min at room temperature and the luminescent signal was measured using a Packard/Perkin-Elmer TopCount. For measurement of apoptosis, BT-474 and SK-BR-3 were exposed to trastuzumab or trastuzumab-MCC-DM1 for 48 h. Caspase activation was assessed by adding Caspase-Glo 3/7 reagent (Promega Corp.) for 30 min at room temperature, and the luminescence was recorded using a Packard TopCount. Induction of cytotoxicity was assessed in cells treated with trastuzumab or trastuzumab-MCC-DM1 for 72 h using ToxiLight Bioassay kit (Cambrex/Lonza). This assay measures release of the intracellular enzyme adenylate kinase as a result of cell lysis.

Normal HMEC and NHEK were plated in clear 96-well plates at densities of 10,000 and 8,000 cells per well, respectively, and allowed to adhere overnight. Cells were treated with trastuzumab or trastuzumab-MCC-DM1 for 72 h. Alamar Blue reagent (Trek Diagnostics Systems) was added to all wells, plates were incubated for 3 h at 37°C, and fluorescence was measured on a SpectraMax 190 (Molecular Devices) using 530-nm excitation and 590-nm emission. Because the normal cell lines were not healthy when grown in black multiplates (which is necessary for use of Cell Titer-Glo), Alamar Blue was used as the proliferation read-out. For all cellular assays, dose-response curves were generated using Kaleidagraph 4.0 (Synergy Software) four-parameter curve fitting.

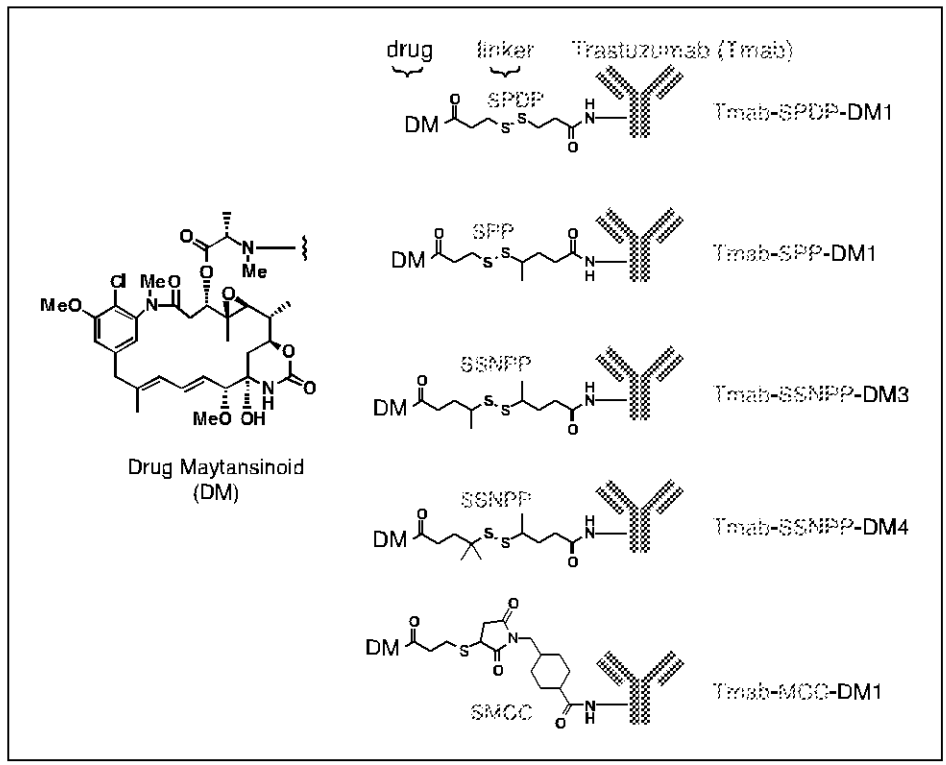

Figure 1. Structure of trastuzumab (Tmab)–maytansinoid conjugates (stability of linker, least to greatest): Tmab-SPDP-DM1, Tmab-SPP-DM1, Tmab-SSNPP-DM3, Tmab-SSNPP-DM4, and Tmab-SMCC-DM1 (nonreducible).

Western immunoblot analysis. SK-BR-3 cells were seeded at a density of 1 million per dish in 100 × 15 mm dishes and allowed to adhere for 2 d. The medium was then removed and replaced with fresh medium containing either trastuzumab, free DM1, or a range of concentrations of trastuzumab-MCC-DM1. After a 48-h incubation, floating cells were collected and combined with detached adherent cells. The total cell population was then centrifuged and resuspended in lysis buffer [50 mmol/L HEPES (pH 7.5), 150 mmol/L NaCl, 1.5 mmol/L $MgCl_2$, 1.0 mmol/L EGTA, 10% glycerol, 1% Triton X-100, 10 mmol/L $Na_4P_2O_4$, 1 mmol/L Na_3VO_4, 50 mmol/L NaF, 1 μmol/L leupeptin, 0.3 μmol/L aprotinin, 1 μmol/L pepstatin A, 10 μmol/L bestatin, and 1.4 μmol/L E-64]. Lysates were cleared by centrifugation at 4°C for 15 min at 20,800 × *g* in a microcentrifuge, and protein concentrations were determined using the bicinchoninic acid (BCA) protein assay kit (Pierce). Proteins were resolved by SDS-PAGE, transferred to nitrocellulose, and immunoblotted with a polyclonal antibody against poly(ADP-ribose) polymerase (PARP), which recognizes intact 116-kDa PARP and the 23-kDa cleavage fragment (R&D Systems). Blotting was carried out in TBS containing 0.1% Triton X-100 and 5% nonfat dry milk, followed by incubation with horseradish peroxidase (HRP)–conjugated secondary antibodies (Amersham Biosciences). Proteins were visualized using enhanced chemiluminescence reagents (Amersham Biosciences).

Measurement of total and phosphorylated HER2 and p95HER2 in transgenic tumors was performed as follows. Tumors from the founder 5 (Fo5; ref. 35) and founder 2#1282 (F2#1282) lineages of MMTV-HER2 transgenic mice (Genentech, Inc.) were excised from the animals, placed in lysis buffer containing protease inhibitors, and homogenized on ice. Tumor lysates were centrifuged, and total protein levels in the supernatant were determined using a BCA protein assay kit. HER2 was immunoprecipitated overnight at 4°C using the mouse monoclonal antibody Ab-15 (Lab Vision) complexed to protein A/G sepharose, with 1 mg total protein from at least three independent tumor lysates. Complexes were pelleted by centrifugation, washed twice with lysis buffer, resuspended in SDS sample buffer, and boiled. Samples were separated on a 4% to 12% Tris-glycine gel and transferred to nitrocellulose membranes. Blots were probed with mouse monoclonal antibody Ab-18 (Lab Vision) to detect the phosphorylated forms of HER2 and p95HER2 or with Ab-15 to detect total HER2 and p95HER2.

***In vivo* efficacy and pharmacokinetic studies.** Tumor tissue from Fo5 or F2#1282 HER2 transgenic mice was collected aseptically, rinsed in HBSS, and cut into pieces of ~2 × 2 mm in size. These pieces were surgically transplanted into the mammary fat pad of female nu/nu mice (Charles River Laboratories). For efficacy studies using BT474EEI cells, naive female beige nude XID mice (Harlan Sprague-Dawley) were inoculated in the mammary fat pad with 20 million tumor cells suspended in 50% phenol red–free Matrigel (Becton Dickinson Bioscience) mixed with culture medium. All animals were randomly assigned into treatment groups, such that the mean tumor volume for each group was 100 to 200 mm^3. Trastuzumab or trastuzumab-maytansinoid conjugates were given by either a single i.v. injection or injection once every 3 wk. Vehicle control was either PBS (for pharmacokinetic studies) or ADC formulation buffer [10 mmol/L sodium succinate, 0.1% polysorbate (Tween) 20, 20 mg/mL trehalose dihydrate (pH5.0)]. Similarly, KPL-4 human breast tumor cells were inoculated (3 million cells per mouse, in Matrigel) into the mammary fat pads of SCID beige mice (Charles River Laboratories). Trastuzumab (15 mg/kg) was given i.p. once per week for 4 wk; trastuzumab-MCC-DM1 (15 mg/kg) was given i.v. (single injection on treatment day 0). All treatment groups consisted of 6 to 10 animals per group, and tumor size was monitored twice weekly using caliper measurement. Mice were housed in standard rodent microisolator cages. Environmental controls for the animal rooms were set to maintain a temperature of ~70°F, a relative humidity of 40% to 60%, and an approximate 14-h light/10-h dark cycle.

For pharmacokinetic analysis of trastuzumab-maytansinoid conjugates, female beige nude mice (age 15–20 wk; Harlan Sprague-Dawley) were injected i.v. with 2 mg/kg of different trastuzumab ADCs (four mice per group). To assess circulating levels of total and conjugated antibody, blood was collected via cardiac puncture from three animals at 5 min and 1, 6, 24, 72, and 168 h postinjection. The samples were left at room temperature for 30 min until the blood coagulated. Subsequently, serum was obtained by centrifuging the samples at 10,000 × *g* for 5 min at 4°C, after which serum samples were stored at −70°C. Total trastuzumab concentration in the serum samples was measured as follows: 96-well ELISA plates were coated with HER2 ECD in 0.05 mol/L carbonate/bicarbonate buffer (pH 9.6) at 4°C overnight. After removal of the coat solution, nonspecific binding sites were blocked by incubating with blocking solution [0.5% bovine serum albumin (BSA) in PBS] for 1 to 2 h. The plates were then washed with wash buffer (0.05% Tween in PBS), and standards or samples diluted in ELISA assay buffer [PBS containing 0.5% BSA, 0.05% Tween, 10 ppm proclin 300, 0.2% bovine γ-globulin, 0.25% CHAPS, 0.35 mol/L NaCl, 5 mmol/L EDTA (pH 7.4)] were added. After a 2-h incubation, plates were washed and HRP-conjugated goat anti-human Fc (The Jackson Laboratory) was added for an additional 2 h. Plates were then washed again, followed by the addition of tetramethyl benzidine substrate for color development. The reaction was stopped after 10 to 15 min by the addition of 1 mol/L phosphoric acid. Plates were read on a Molecular Devices microplate reader at a wavelength of 450 to 630 nm. The concentration of trastuzumab in the samples was extrapolated from a four-variable fit of the standard curve. For measurement of trastuzumab-maytansinoid concentration, wells were coated with anti-DM antibody (GNE DM1-3586) and serum samples added as above. After the 2-h sample incubation, the plates were washed, 60 ng/mL biotin-conjugated HER2 ECD was added to each well, and the plates were incubated for 1 h. Plates were then washed, and HRP-conjugated streptavidin (GE Healthcare) was added for an additional 30-min incubation. Color detection and measurement were performed as described above. Previous analyses of different preparations of trastuzumab-DM1 conjugates with drug-antibody ratios ranging from 1.9 to 3.8 showed that the conjugated antibody ELISA is not sensitive to drug load.

Circulating HER2 ECD levels from mice harboring Fo5 or F2#1282 xenograft tumors was measured, as previously described (35). Briefly, serum was diluted 1:50 with ELISA assay buffer (above) followed by 1:2 serial dilutions. HER2 ECD was captured using goat anti-HER2 polyclonal antibody (Genentech, Inc.) and detected with biotin-conjugated rabbit anti-Her2 polyclonal (Genentech, Inc.), followed by addition of streptavidin-HRP.

Rat toxicity studies. Female Sprague-Dawley rats weighing 75 to 80 g were obtained from Charles River Laboratories and allowed to acclimate for 5 d before study. Trastuzumab-SPP-DM1, trastuzumab-MCC-DM1, and free DM1 were diluted in PBS (Invitrogen Corp.) as vehicle and given as a single i.v. bolus tail-vein injection on day 1 at a dose volume of 10 mL/kg. Body weights were measured predose on day 1 and daily thereafter for 5 d.

Results

Linker optimization. Antibody-DM1 conjugates were originally designed with a disulfide-based linker for release of active drug by intracellular reduction (24). Recently, it was discovered that the endocytic pathway is oxidizing and that cleavage of the disulfide linker, SPP, is very inefficient (36). Thus, different trastuzumab ADCs were constructed to investigate the effect of disulfide linker hindrance on the biological activity of these conjugates (Fig. 1). A trastuzumab-DM1 conjugate made with the SPDP linker contains no methyl substitutions adjacent to the disulfide bond and is therefore the least hindered disulfide-containing design. Trastuzumab ADCs composed of SPP-DM1, SSNPP-DM3, or SSNPP-DM4 contain one, two, or three methyl groups, respectively, around the disulfide bridge and show increasing resistance to cleavage via thiol-disulfide exchange reactions.[3] DM3 and DM4 nomenclature

[3] ImmunoGen, Inc., unpublished data.

reflects addition of methyl groups to the DM1 (drug) moiety (addition of one or two methyls, respectively). An additional ADC containing a thioether linker (SMCC, designated MCC after conjugation) was also constructed. *In vitro* potency assays were conducted for 3 days with the HER2-amplified breast cancer lines BT-474 and SK-BR-3 treated with various trastuzumab ADCs. This short treatment period was selected to minimize the effects of unconjugated trastuzumab on these trastuzumab-sensitive lines. The graphs in Fig. 2*A* show enhanced potency of trastuzumab-maytansinoid conjugates compared with trastuzumab in both cell lines, with no significant difference in activity among the various ADCs tested (IC_{50}, 0.085–0.148 μg/mL for BT-474 and 0.007–0.018 μg/mL for SK-BR-3). Because the effect of trastuzumab is cytostatic in nature, the enhanced potency of the ADC is, thus, due to exposure of the cells to the cytotoxic maytansinoid. In addition, brief exposure of SK-BR-3 cells for 10, 30, or 60 minutes to trastuzumab-MCC-DM1, followed by a 3-day incubation in culture medium, also resulted in substantial growth inhibition (data not shown). When comparing potency as molar DM1 equivalents, DM1 conjugated to trastuzumab is 5-fold more potent than free L-DM1 on SK-BR-3 and shows equal potency to free L-DM1 on BT-474 cells (Fig. 2*B*). Nontargeted effects of trastuzumab-maytansinoid conjugates were assessed on breast cancer lines expressing normal levels (MCF7) or lacking expression (MDA-MB-468) of HER2 (37). All ADCs tested showed minimal antiproliferative activity in both cell lines (Fig. 2*A*), whereas free DM1 showed potency equal to that observed on the HER2-amplified lines (Fig. 2*B*). Treatment of the four cell lines with an isotype-matched control ADC, anti–IL-8-MCC-DM1, resulted in negligible growth inhibition (data not shown). Thus, like trastuzumab, maytansinoid-conjugated trastuzumab ADCs are specific for HER2-overexpressing cells. Furthermore, the different linkers behave similarly with respect to *in vitro* antiproliferative activity.

Pharmacokinetic analyses in nude mice were performed to determine the effect of different trastuzumab ADC linkers on serum concentration. In contrast to the cell culture results, we observed a clear correlation between ADC exposure and linker hindrance. The ADC with the least hindered disulfide bond (no adjacent methyl groups), trastuzumab-SPDP-DM1, showed the fastest clearance and was undetectable by day 3. The addition of methyl groups (CH_3) on either side of the S-S bond (trastuzumab-SPP-DM1 with one CH_3 on the antibody side of the S-S; trastuzumab-SSNPP-DM3 with two CH_3, one on either side of the S-S; trastuzumab-SSNPP-DM4 with three CH_3, one on the antibody side, and two on the drug side of the S-S) resulted in increasingly sustained ADC serum concentrations (Fig. 3*A*, *left*). Trastuzumab-MCC-DM1 (nonreducible) and trastuzumab-SSNPP-DM4 (the most hindered disulfide-containing design) showed similar pharmacokinetics with the ADC concentration at 70% of the total antibody at day 7. Studies were also performed to compare clearance of DM1-conjugated trastuzumab to total trastuzumab levels (Fig. 3*A*, *right*). Serum concentrations of trastuzumab-MCC-DM1 measured for 1 week were not different from total serum trastuzumab concentration, indicating that, with the nonreducible MCC linker, the amount of maytansinoid released from the antibody was negligible over the 7 days. In contrast, only 11% of the trastuzumab-SPP-DM1, compared with total trastuzumab antibody concentration, remained in the circulation after 7 days.

In vivo efficacy studies examining the different trastuzumab-maytansinoid conjugates given as a single i.v. dose were carried out using the MMTV-HER2 Fo5 mammary tumor transplant (trastuzumab-resistant) model. This model was developed by serial transplantation of tumors derived from the HER2 transgenic mouse lineage founder 5 (35). These mouse tumors overexpress human HER2 (3+ expression) as measured by immunohistochemistry and quantitative reverse transcription–PCR. Interestingly, established tumors from this model do not respond to single-agent trastuzumab therapy. Consistent with the pharmacokinetic analysis, increased linker stability *in vivo* correlated with increased antitumor activity for trastuzumab ADCs (Fig. 3*B*). Tumor volume in both trastuzumab-MCC-DM1 and trastuzumab-SSNPP-DM3 treatment groups were statistically different from trastuzumab-SPP-DM1 (log-rank P values of 0.0165 and 0.0414, respectively). Further characterization of the HER2 transgenic models revealed the presence of high circulating levels of shed HER2 ECD in the serum of Fo5 tumor-bearing mice. Moreover, analysis of these tumors revealed increased expression of the transmembrane-containing fragment p95HER2, which is highly tyrosine-phosphorylated, indicating constitutive activation. In comparison, the trastuzumab-sensitive F2#1282 model showed 1,000-fold lower levels of circulating HER2 ECD, no detectable p95HER2, and significant tumor growth reduction after a single injection of different doses of trastuzumab-DM1 (data not shown). Thus, the trastuzumab-DM1 conjugate is efficacious in models, such as Fo5, which express reported markers of resistance to trastuzumab, i.e., high circulating HER2 ECD and activated p95HER2.

Short-term, single-dose toxicity studies were performed in female rats comparing the effects on body weight of free or conjugated (SMCC or SPP) DM1. ADCs were given as DM1 equivalents (μg/m^2). As trastuzumab does not recognize rat erbB2, this model measures antigen-independent ADC effects. Of the agents tested, trastuzumab-MCC-DM1 showed the best safety profile. Body weight gain in rats given 1,632 μg/m^2 DM1 (25 mg/kg antibody) was comparable with vehicle control animals (15.9% and 16.3%, respectively; Fig. 3*C*). In contrast, administration of trastuzumab-SPP-DM1 at an equivalent DM1 dose resulted in considerable body weight loss (−10%) by end of study. Rats treated with 3,264 μg/m^2 (50 mg/kg) trastuzumab-MCC-DM1 did not exhibit body weight loss; however, the amount of weight gained during the course of study (+6.7%) was less than in the vehicle control and the 1,632 μg/m^2 trastuzumab-MCC-DM1 groups. The change in body weight with 3,264 μg/m^2 trastuzumab-MCC-DM1 was similar to that observed with free DM1 at a dose of 653 μg/m^2 (+6.5%). In a separate study, clinical chemistry analysis of rats treated with trastuzumab-MCC-DM1 showed transient elevation of liver enzymes (aspartate aminotransferase, alanine aminotransferase, and γ-glutamyl transpeptidase) and mild, reversible thrombocytopenia at a dose of 20 mg/kg, and no clinical signs of toxicity at 6 mg/kg (data not shown). Evidently, substituting a reducible linker (SPP) with a nonreducible linker (SMCC) results in a less toxic but still efficacious trastuzumab-DM1 conjugate. Consequently, further studies focused on defining the activity of trastuzumab-MCC-DM1.

HER2-overexpressing, trastuzumab-resistant tumor cells respond to trastuzumab-MCC-DM1, whereas normal cell lines are unaffected. The effects of trastuzumab-MCC-DM1 on *in vitro* proliferation were further examined in several tumor lines shown to be resistant to trastuzumab. Additional breast cancer lines, HCC1954, KPL-4, and BT-474 EEI, all with 3+ HER2 expression, were first tested. The BT-474 EEI cell line was developed by

A

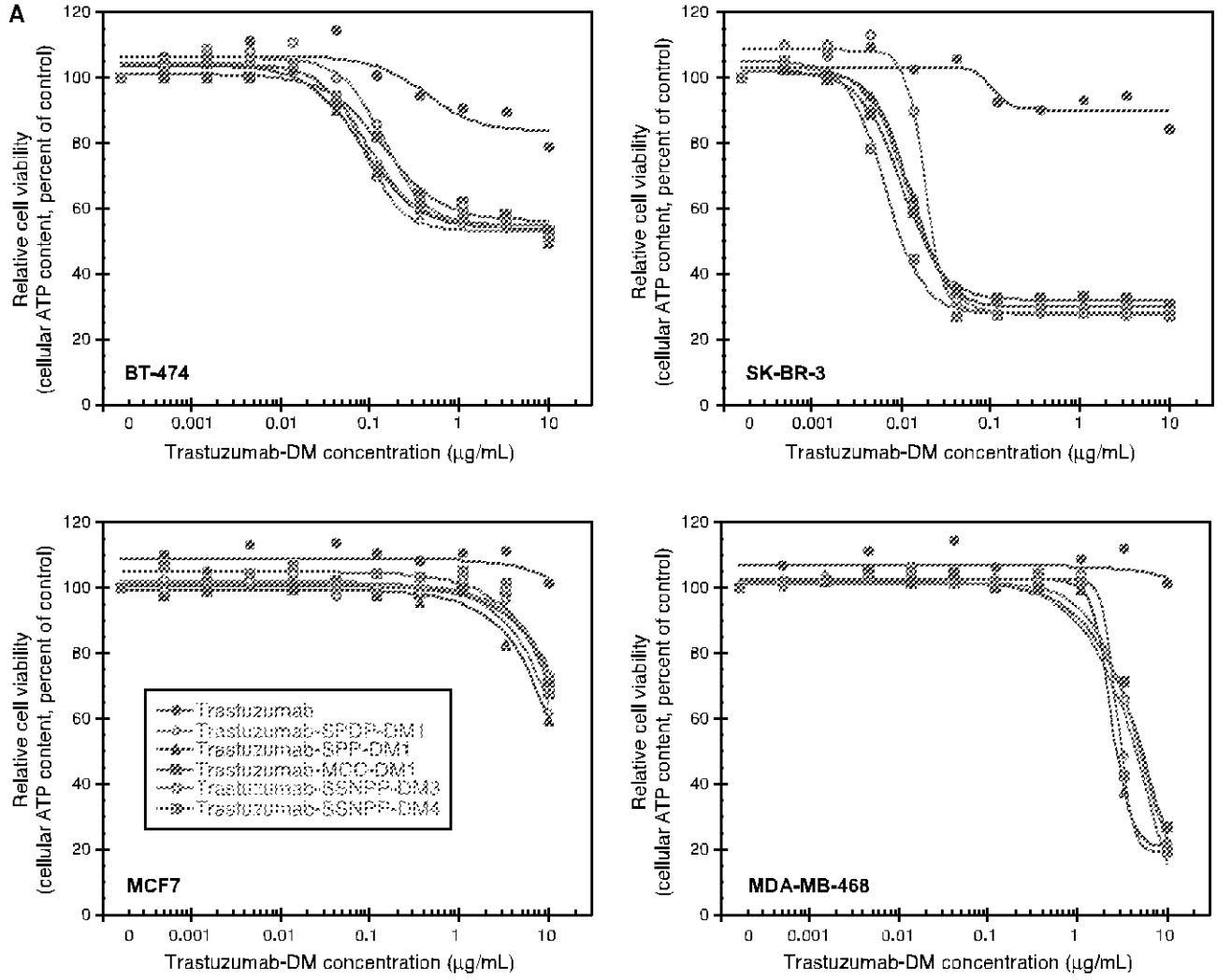

B

***In vitro* activity of trastuzumab-DM1 conjugates versus free DM1 (IC_{50}, nmol/L DM1 equivalents)**

	trastuzumab-SPP-DM1	trastuzumab-MCC-DM1	free L-DM1
SK-BR-3	0.24	0.22	1.00
BT-474	2.71	4.26	4.52
MCF7	>100	>100	2.92
MDA-MB-468	18.37	41.37	0.59

Cells were treated with trastuzumab-DM1 conjugates or L-DM1 as free drug for 72 h; IC_{50} values were determined from four-parameter curve fitting.

Figure 2. Trastuzumab-maytansinoid conjugates are selective for HER2-amplified breast cancer lines, whereas free DM1 shows equivalent potency on all cell lines tested regardless of HER2 expression. *A,* trastuzumab-maytansinoid conjugates show enhanced antiproliferative activity on HER2-overexpressing breast tumor cell lines compared with trastuzumab. The nature of the linker, however, does not affect *in vitro* activity. *B, in vitro* potency of Tmab-SPP-DM1 and Tmab-MCC-DM1 compared with the free drug L-DM1 after 3 d of treatment (IC_{50} values, nmol/L DM1 equivalents). HER2 expression: SK-BR-3 (HER2 3+), BT-474 (HER2 3+), MCF7 (normal HER2 expression), MDA-MB-468 (HER2-negative).

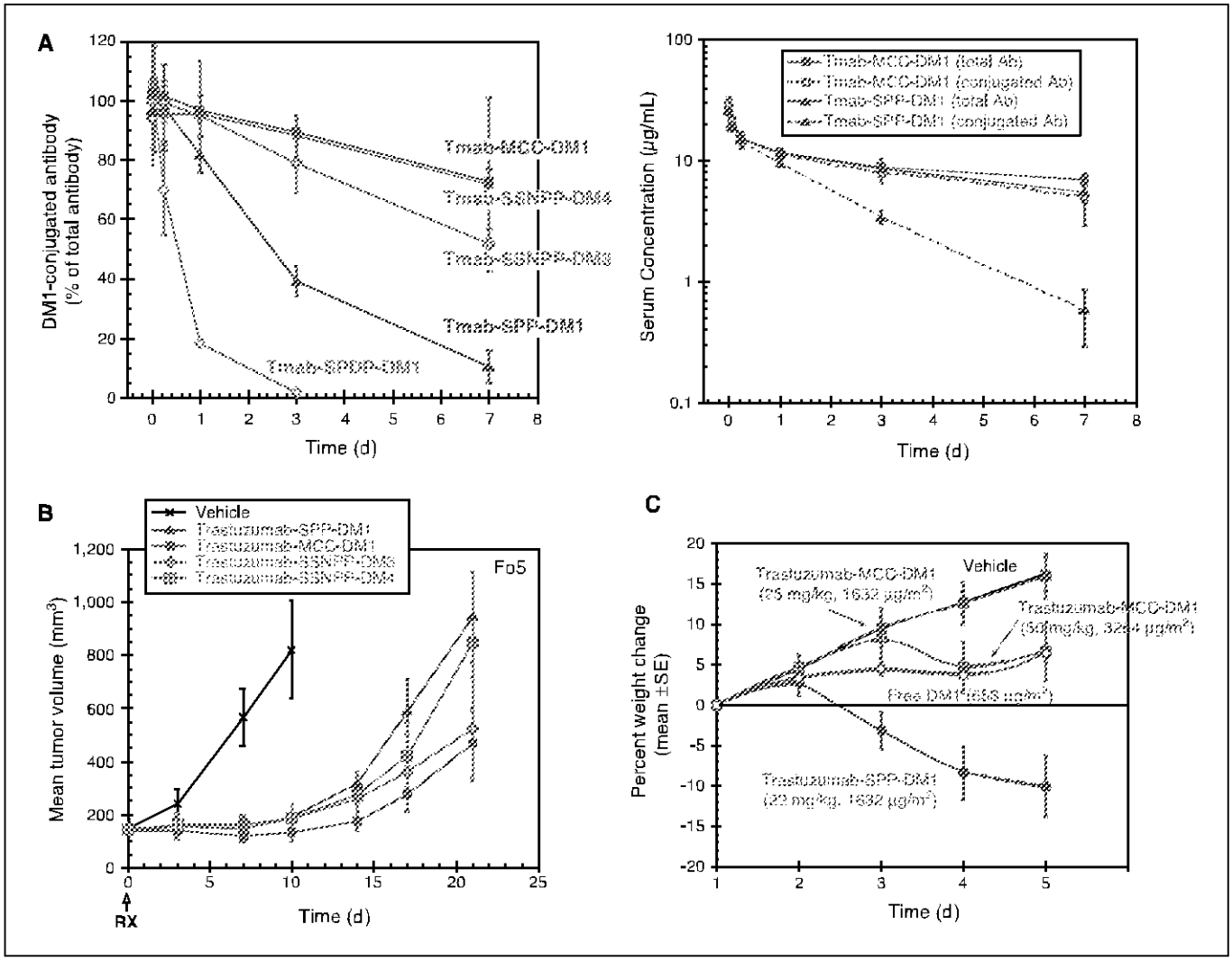

Figure 3. Trastuzumab conjugated to DM1 through the thioether SMCC linker displays better efficacy and pharmacokinetics and lower toxicity than conjugates with disulfide linkers. *A,* pharmacokinetic analysis of trastuzumab-maytansinoid conjugates shows increased serum concentrations of conjugates with more hindered disulfide linkers. Female beige nude mice were given a single i.v. injection (2 mg/kg) of different trastuzumab-maytansinoid conjugates (n = 4 mice per group). Serum samples were collected at various time points after injection for measurement of total and conjugated trastuzumab as described. *B,* increased *in vivo* linker stability results in improved efficacy *in vivo*. Mice bearing mammary tumor transplants from the MMTV-HER2 Fo5 line were given a single i.v. injection (10 mg/kg) of Tmab-SPP-DM1, Tmab-SSNPP-DM3, Tmab-SSNPP-DM4, Tmab-MCC-DM1, or vehicle (n = 7 mice per group), and tumor growth was monitored for 25 d. *C,* Tmab-MCC-DM1 displays the best safety profile, as assessed by changes in body weight, of the conjugates tested. Female Sprague-Dawley rats were given a single i.v. injection of Tmab-MCC-DM1 (1,632 or 3,264 μg/m^2, 25 or 50 mg/kg, respectively), Tmab-SPP-DM1 (1,632 μg/m^2), or free DM1 (653 μg/m^2) on day 1, and body weights were measured daily for 5 d. To give equivalent doses of DM1, animals in the Tmab-SPP-DM1 group were given 22 mg/kg due to the higher drug-antibody ratio (3.6) compared with Tmab-MCC-DM1 (3.2).

subculturing BT-474 tumors grown *in vivo* in the absence of estrogen pellet supplementation. The cell line established in this manner, while maintaining high levels of HER2 expression, had surprisingly become resistant to trastuzumab (G.P. and L.C.) and provides a useful model for determining efficacy of trastuzumab ADCs. These three breast cancer lines showed the same degree of sensitivity to trastuzumab-MCC-DM1 as the sensitive lines SK-BR-3 and BT-474 (Fig. 4*A*). Moreover, tumor lines from different tissues of origin were also responsive to treatment with trastuzumab-MCC-DM1. Calu 3 lung carcinoma (3+ HER2), SK-OV-3 ovarian carcinoma (2+ HER2), and MKN7 gastric carcinoma (2+ HER2) cells (37) displayed dose-dependent inhibition of cell growth upon treatment with the ADC while showing no response to nonconjugated trastuzumab (Fig. 4*B*). In contrast, exposure of normal human cells, HMEC and NHEK, to trastuzumab-MCC-DM1 resulted in minimal growth inhibition, similar to that observed on HER2 nonamplified MCF-7 and MDA-MB-468 breast carcinoma cells (Fig. 4*C*).

Trastuzumab-MCC-DM1 induces cell death in HER2-overexpressing breast cancer cells. Further studies were performed to address the mechanism(s) of action of trastuzumab-MCC-DM1. Cell cycle analysis of conjugate-treated cells resulted in the expected arrest in the G_2-M phase (data not shown), a known mechanism of agents that inhibit microtubule function. We examined the effects on cell death induction, as well. Trastuzumab-MCC-DM1 induced a dose-dependent increase in cell death in SK-BR-3 and BT-474 cells (Fig. 5), with EC_{50} values (in parentheses) similar to those observed in proliferation assays. Release of the

intracellular enzyme adenylate kinase into the culture medium, an indicator of cellular lysis, was observed after treatment with trastuzumab-MCC-DM1 for 3 days (Fig. 5*A*). Activation of caspase-3/caspase-7 also occurred in these cell lines after a 2-day treatment with trastuzumab-MCC-DM1, indicating induction of apoptotic cell death (Fig. 5*B*). Proteolytic cleavage of 116-kDa PARP with release of the 23-kDa fragment, a known hallmark of apoptotic cell death, was also examined. PARP cleavage was observed in SK-BR-3 cells treated for 48 hours with 100 and 300 ng/mL trastuzumab-MCC-DM1, as well as with 20 nmol/L free DM1, indicating induction of

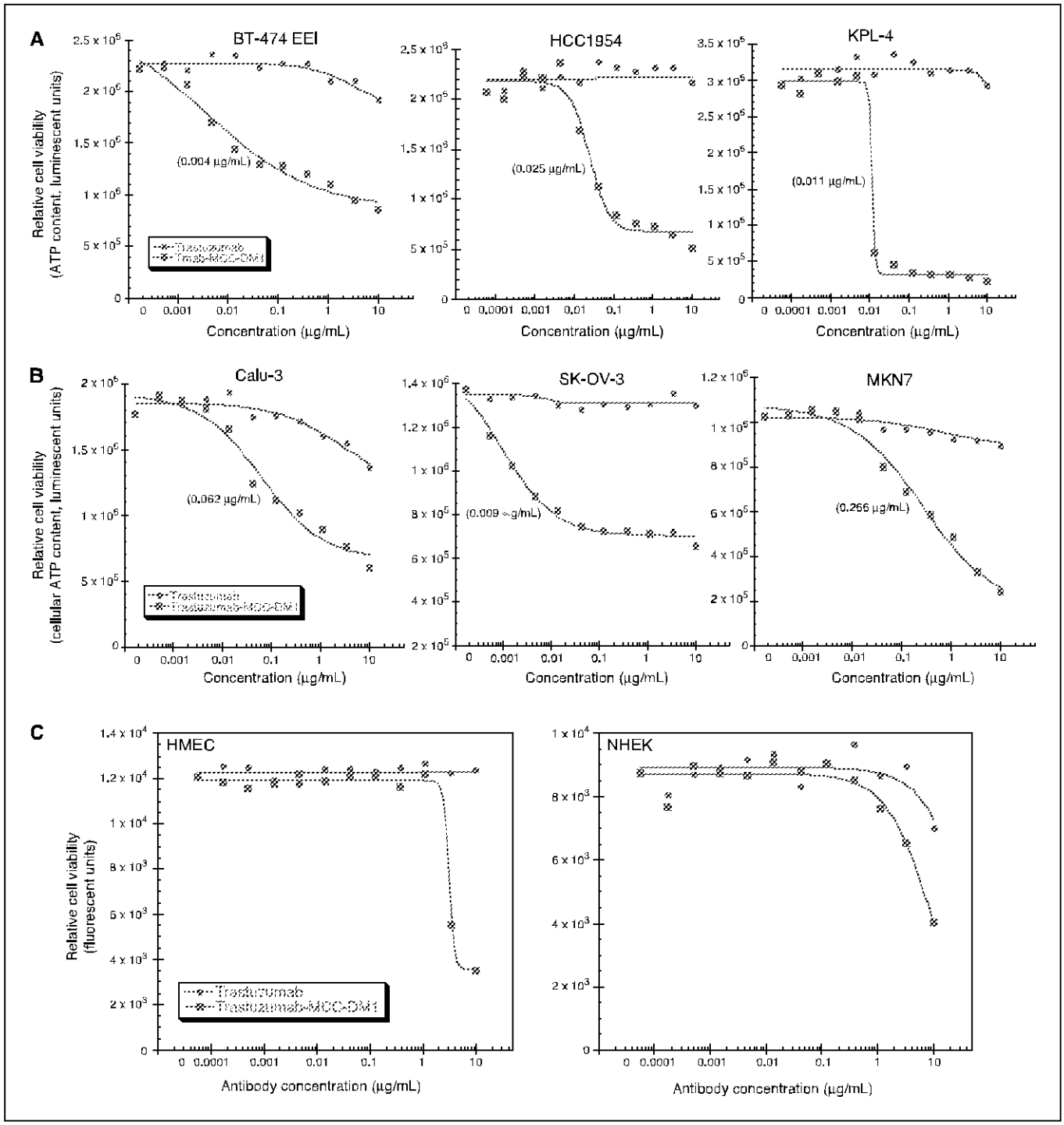

Figure 4. Trastuzumab-MCC-DM1 induces a potent antiproliferative effect in trastuzumab-resistant tumor cells but has no effect on normal human cells. *A,* breast tumor lines BT-474 EEI, HCC1954, and KPL-4 (all HER2 3+). *B,* Calu-3 lung carcinoma (HER2 3+), SK-OV-3 ovarian carcinoma, and MKN7 gastric carcinoma (both HER2 2+). *C,* normal cells HMEC and NHEK were all treated with either trastuzumab or trastuzumab-MCC-DM1 for 3 d, and relative proliferation was determined using CellTiter-Glo. IC_{50} values for each cell line are in parentheses.

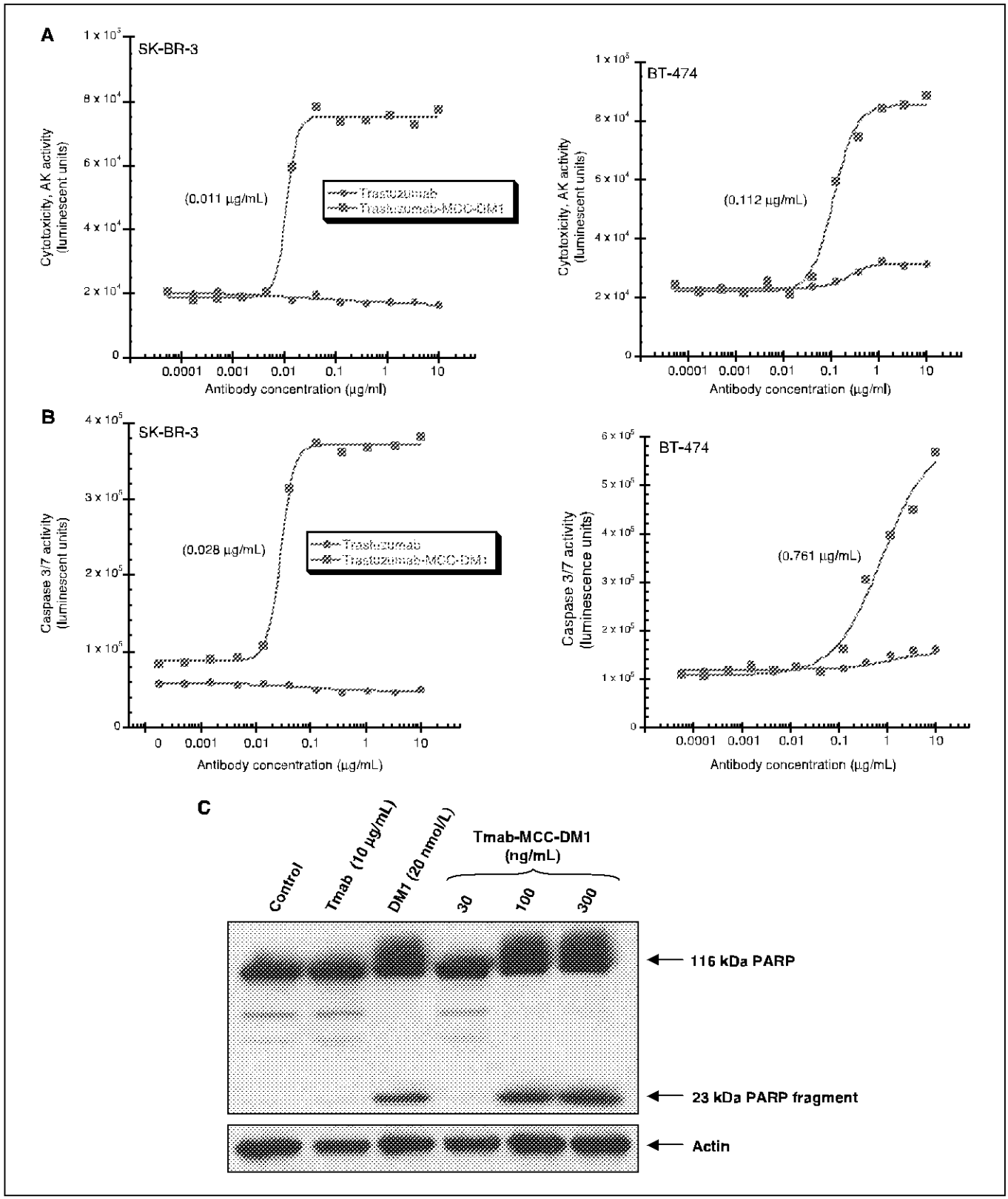

Figure 5. Trastuzumab-MCC-DM1, but not trastuzumab, induces cell lysis and apoptosis in SK-BR-3 and BT-474 breast tumor cells. Cytotoxic response (*A*), as measured by adenylate kinase release into the culture medium, and apoptosis induction (*B*), measured by activation of caspase-3/caspase-7, after treatment with trastuzumab or trastuzumab-MCC-DM1 for 3 d (cytotoxicity) or 2 d (caspase-3/caspase-7 activation). EC_{50} values are shown in parentheses. *C,* trastuzumab-MCC-DM1 and free DM1 induce PARP cleavage, whereas unconjugated trastuzumab has no effect. SK-BR-3 cells were treated with 10 μg/mL trastuzumab; 30, 100, or 300 ng/mL Tmab-MCC-DM1 (0.02, 0.67, and 2.0 nmol/L, respectively) or 20 nmol/L free DM1 for 48 h. Cells were then lysed for Western blot analysis of cleaved PARP. Appearance of the 23-kDa PARP fragment indicates apoptotic activation of PARP cleavage.

apoptosis (Fig. 5*C*). Thus, in contrast to the cytostatic action of trastuzumab (7, 30), these data show that treatment of HER2-amplified breast tumor cells with trastuzumab-MCC-DM1 results in apoptotic cell death and cellular lysis.

Trastuzumab-MCC-DM1 inhibits growth and causes tumor regression in animal models of HER2-positive breast cancer. The *in vivo* efficacy of trastuzumab-MCC-DM1 was compared with trastuzumab in three mouse models of HER2-overexpressing breast cancer. KPL-4 human breast tumor cells were implanted into the mammary fat pads of SCID beige mice and tumors allowed to grow to an average size of 300 mm^3. Mice were then treated weekly with 15 mg/kg trastuzumab i.p. or given a single i.v. injection of 15 mg/kg trastuzumab-MCC-DM1. Complete tumor regression for the duration of the study (126 days), as determined by caliper measurement, was observed in mice receiving trastuzumab-MCC-DM1, whereas unconjugated trastuzumab induced an initial decrease in tumor size, followed by regrowth upon cessation of treatment (Fig. 6*A*). Although the KPL4 cell line did not respond to trastuzumab *in vitro*, we have observed with other cell lines, such as Calu 3, response to trastuzumab *in vivo*, despite lack of responsiveness *in vitro*.

The activity of trastuzumab-MCC-DM1 was further investigated in two trastuzumab-insensitive mouse xenograft models. After transplantation of MMTV-HER2 Fo5 mammary tumor explants,

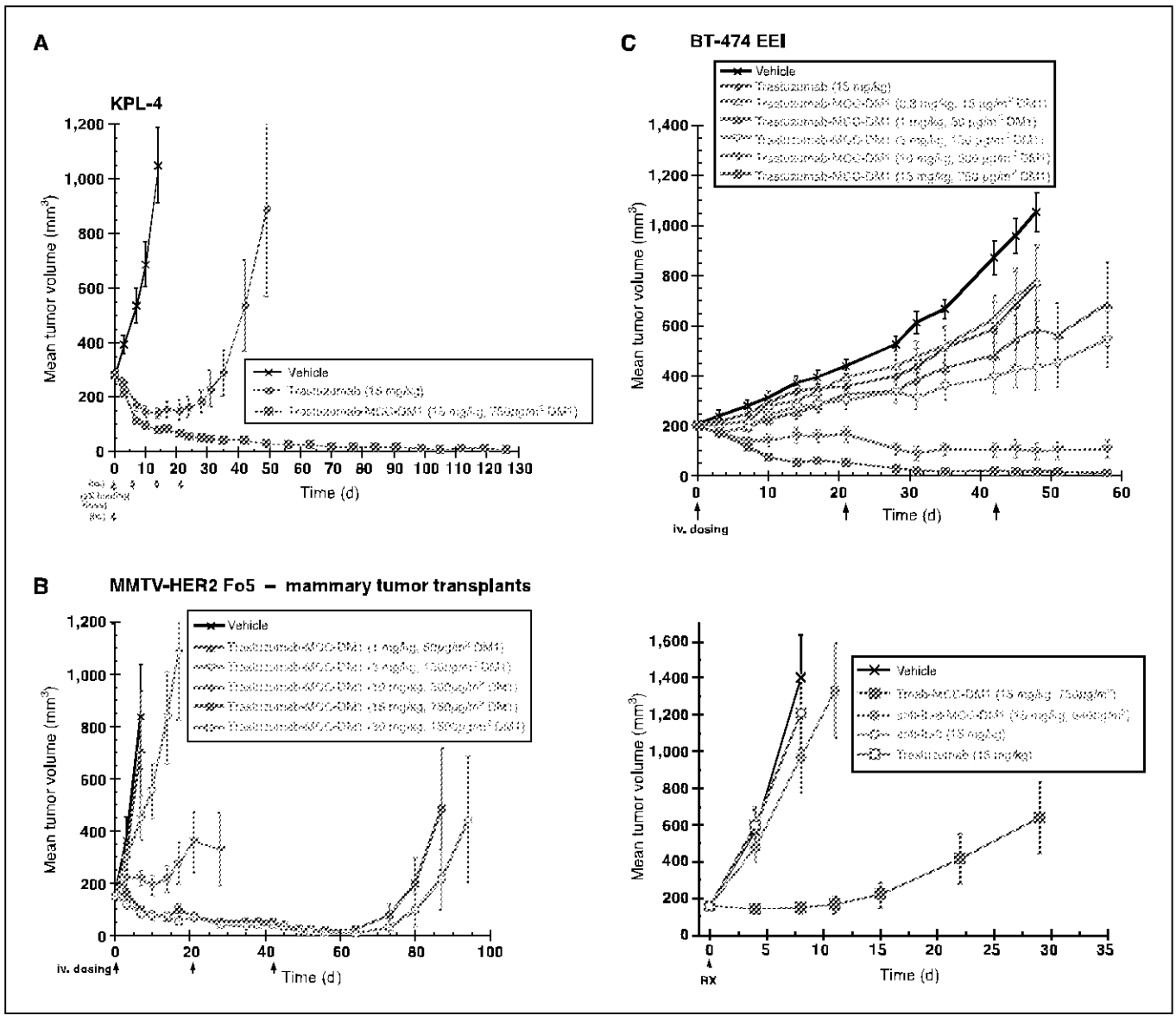

Figure 6. *In vivo* efficacy of trastuzumab-DM1 in trastuzumab-sensitive and trastuzumab-resistant breast tumor models. *A,* KPL-4 human breast cancer cells grown as tumors in SCID beige mice show complete regression after a single i.v. injection of trastuzumab-MCC-DM1 (15 mg/kg, 750 μg/m^2 DM1) compared with transient regression followed by regrowth after weekly treatment with 15 mg/kg trastuzumab (n = 8 mice per group). *B,* MMTV-HER2 transgenic transplants from trastuzumab-resistant line Fo5 respond to trastuzumab-MCC-DM1 in a dose-dependent manner (*left*). Injections were given once every 3 wk for three total injections at doses of 1, 3, 10, 15, and 30 mg/kg (50, 150, 500, 750, and 1,500 μg/m^2 DM1, respectively); n = 8 mice per group. Isotype-matched control ADC, anti–IL-8-MCC-DM1 (15 mg/kg, 840 μg/m^2 DM1; drug-antibody ratio, 3.8) showed no antitumor activity (*right*). *C,* dose-response of trastuzumab-resistant xenograft line BT-474 EEI to trastuzumab-MCC-DM1. Nude mice with established tumors were dosed i.v. with Tmab-MCC-DM1 (0.3, 1, 3, 10, or 15 mg/kg) or with 15 mg/kg trastuzumab once every 3 wk for a total of three injections, n = 10 mice per group.

tumor-bearing nude mice were treated once every 3 weeks with 1, 3, 10, 15, or 30 mg/kg trastuzmab-MCC-DM1 (50, 150, 500, 750, and 1500 $\mu g/m^2$ of conjugated DM1, respectively; Fig. 6*B*). Doses of 1 and 3 mg/kg showed no antitumor activity, whereas administration of 10 mg/kg resulted in partial inhibition of tumor growth (this treatment group was discontinued after 30 days due to several mice having tumors in excess of 1,000 mm^3). Tumors in mice treated with either 15 or 30 mg/kg trastuzumab-MCC-DM1 regressed during the entire course of treatment. Regrowth was observed ~30 days after discontinuation of treatment. Previous studies have shown that retreatment with trastuzumab-MCC-DM1 results in a further decrease in tumor size, indicating that acquisition of resistance did not occur (data not shown). In contrast, treatment with 15 mg/kg of an irrelevant control ADC, anti-IL-8-MCC-DM1, resulted in no tumor growth inhibition (Fig. 6*B*, *right*).

The second trastuzumab-resistant model used the BT-474 EEI tumor-derived line. The data in Fig. 6*C* show the effects on BT-474 EEI tumor growth of different doses of trastuzumab-MCC-DM1 given once every 3 weeks for three total doses. Dose-dependent inhibition of tumor growth was observed, with 0.3, 1 and 3 mg/kg causing tumor growth delay, whereas 10 and 15 mg/kg doses resulted in tumor regression. Thus, trastuzumab-MCC-DM1 shows potent activity in trastuzumab-sensitive and trastuzumab-insensitive mouse xenograft models, with 15 mg/kg as the maximum efficacious dose.

Discussion

The anatomy of an antibody–cytotoxic drug conjugate can be divided into three general components: the antibody, the linker, and the cytotoxic drug. The efficacy of any such conjugate is dictated in part by the differential expression of the target antigen in tumor versus normal tissue. HER2 is a clinically validated target for the treatment of breast cancer. Trastuzumab (5, 35–41) and, more recently, lapatinib (42) are approved for clinical use in women whose breast cancer overexpresses HER2. To be maximally effective, both trastuzumab and lapatinib require a functional or signaling HER2 receptor, which drives key biological aspects of the tumor. It is postulated that patients whose tumors progress on these therapies may acquire alterations that activate signal transduction pathways either downstream or parallel to HER2. At present, available data indicate that cancer cells do not lose HER2 expression when they become refractory to HER2-directed therapies (14, 16). For that reason, a trastuzumab conjugate, which simply uses HER2 as an address for the delivery of a potent cytotoxic agent, may offer promise as an effective therapeutic modality.

We observed that anti-HER2 ADCs display impressive potency *in vitro* and *in vivo* and are active in trastuzumab-refractory models of HER2-amplified breast cancer. However, the tolerability of these conjugates varies considerably and is intrinsically dependent upon the chemical nature of the linker and the cytotoxic agent. In this report, we describe our characterization of several trastuzumab-maytansinoid conjugates with a special emphasis on linker chemistry. The disulfide-linked DM1-containing ADCs were designed to allow for endosomal reduction of the disulfide to result in intracellular release of the cytotoxic agent. Moreover, in antigen-expressing tumor cells, DM1 derived from ADCs desigued with a disulfide linker can be released by the tumor cells and initiate a "bystander" killing effect (34). However, *in vivo*, the liberated DM1 is also rapidly cleared and, thus, may not be available for prolonged antitumor effects (43). Our results with the thioether (MCC) linker contradicted the hypothesis that selective release of DM1 by intracellular reduction of the disulfide bond in a trastuzumab-disulfide-DM1 conjugate was necessary for efficacy. Similar to huC242-MCC-DM1, a thioether-containing ADC that targets the CanAg antigen (34, 44), trastuzumab-MCC-DM1 is internalized upon binding to HER2-overexpressing tumor cells and is postulated to undergo intracellular proteolytic degradation to release active maytansinoid. As expected, the activity of trastuzumab-MCC-DM1 is blocked in the presence of protease inhibitors in cell culture experiments (data not shown). Subsequently, it has been shown that HER2 itinerary allows for lysosomal degradation of HER2-directed ADCs (45). Thus, it is likely that the trastuzumab antibody component of the trastuzumab-MCC-DM1 conjugate undergoes proteolytic degradation in the lysosome and that lysine-MCC-DM1 is a major active metabolite, as has been shown for huC242-MCC-DM1 (44). In fact, preliminary data from studies investigating the metabolism of [^{3}H]trastuzumab-MCC-DM1 in BT-474 EEI cells show lysine-N^{ϵ}-MCC-DM1 as the predominant metabolite (data not shown). The primary active metabolite, lysine-MCC-DM1, does not readily cross the plasma membranes of neighboring cells and, therefore, does not elicit a bystander effect (34, 44).

Non–disulfide-containing ADCs show increased pharmacokinetic exposure in both rats and cynomolgus monkeys (data not shown). This increase in conjugate exposure did not lead to an increase in either target-dependent or target-independent toxicity. As expected, trastuzumab conjugated to DM1 through the thioether MCC linker was better tolerated compared with the disulfide (SPP) linked to DM1, with regard to toxicity siguals. Despite the improved pharmacokinetic profile of DM3 and DM4-containing trastuzumab conjugates, the disulfide linkage would likely render these conjugates less tolerable than the thioether-linked trastuzumab conjugate.

In summary, trastuzumab-MCC-DM1 is shown to be efficacious in trastuzumab-sensitive and trastuzumab-insensitive models of HER2-overexpressing cancer. Of equal importance, trastuzumab-MCC-DM1 has a favorable pharmacokinetic and safety profile compared with disulfide-linked trastuzumab conjugates and represents an important new approach for treating HER2-amplified human cancers. Given these promising results, early clinical studies are currently under way to assess the safety and efficacy of trastuzumab-MCC-DM1 in patients whose disease has progressed through HER2-directed therapies.

Disclosure of Potential Conflicts of Interest

G.D. Lewis Phillips, G. Li, D.L. Dugger, L.M. Crocker, K.L. Parsons, E. Mai, W. L.T. Wong, F.S. Jacobson, S.R. Kenkare-Mitra, S.D. Spencer, and M.X. Sliwkowski are employees of and shareholders in Genentech, Inc. W.A. Blättler, J.M. Lambert, R.V.J. Chari, and R.J. Lutz are employees of and shareholders in ImmunoGen, Inc. H. Koeppen is a former Genentech, Inc. employee.

Acknowledgments

Received 5/19/2008; revised 7/23/2008; accepted 9/8/2008.

The costs of publication of this article were defrayed in part by the payment of page charges. This article must therefore be hereby marked *advertisement* in accordance with 18 U.S.C. Section 1734 solely to indicate this fact.

This article is dedicated to our dear colleague, Dr. Ralph Schwall, who passed away on August 26, 2005.

We thank Drs. Vishva Dixit, Paul Polakis, Richard Scheller, and Robert Cohen for their support, interest, and valuable discussions; Allison Bruce for graphics support; and Dr. J. Kurebayashi for providing the KPL4 cell line.

References

1. Yarden Y, Sliwkowski MX. Untangling the ErbB signalling network. Nat Rev Mol Cell Biol 2001;2:127–37.
2. Yarden Y. The EGFR family and its ligands in human cancer. Signaling mechanisms and therapeutic opportunities. Eur J Cancer 2001;37 Suppl 4:S3–8.
3. Slamon DJ, Clark GM, Wong SG, Levin WJ, Ullrich A, McGuire WL. Human breast cancer: correlation of relapse and survival with amplification of the HER-2/neu oncogene. Science 1987;235:177–82.
4. Slamon DJ, Godolphin W, Jones LA, et al. Studies of the HER-2/neu proto-oncogene in human breast and ovarian cancer. Science 1989;244:707–12.
5. Slamon DJ, Leyland-Jones B, Shak S, et al. Use of chemotherapy plus a monoclonal antibody against HER2 for metastatic breast cancer that overexpresses HER2. N Engl J Med 2001;344:783–92.
6. Smith I, Procter M, Gelber RD, et al. 2-year follow-up of trastuzumab after adjuvant chemotherapy in HER2-positive breast cancer: a randomised controlled trial. Lancet 2007;369:29–36.
7. Sliwkowski MX, Lofgren JA, Lewis GD, Hotaling TE, Fendly BM, Fox JA. Nonclinical studies addressing the mechanism of action of trastuzumab (Herceptin). Semin Oncol 1999;26:60–70.
8. Hudis CA. Trastuzumab-mechanism of action and use in clinical practice. N Engl J Med 2007;357:39–51.
9. Nahta R, Yu D, Hung MC, Hortobagyi GN, Esteva FJ. Mechanisms of disease: understanding resistance to HER2-targeted therapy in human breast cancer. Nat Clin Pract Oncol 2006;3:269–80.
10. Chan CT, Metz MZ, Kane SE. Differential sensitivities of trastuzumab (Herceptin)-resistant human breast cancer cells to phosphoinositide-3 kinase (PI-3K) and epidermal growth factor receptor (EGFR) kinase inhibitors. Breast Cancer Res Treat 2005;91:187–201.
11. Clark AS, West K, Streicher S, Dennis PA. Constitutive and inducible Akt activity promotes resistance to chemotherapy, trastuzumab, or tamoxifen in breast cancer cells. Mol Cancer Ther 2002;1:707–17.
12. Nagata Y, Lan KH, Zhou X, et al. PTEN activation contributes to tumor inhibition by trastuzumab, and loss of PTEN predicts trastuzumab resistance in patients. Cancer Cell 2004;6:117–27.
13. Lu Y, Zi X, Zhao Y, Mascarenhas D, Pollak M. Insulin-like growth factor-I receptor signaling and resistance to trastuzumab (Herceptin). J Natl Cancer Inst 2001;93:1852–7.
14. Nahta R, Yuan LX, Zhang B, Kobayashi R, Esteva FJ. Insulin-like growth factor-I receptor/human epidermal growth factor receptor 2 heterodimerization contributes to trastuzumab resistance of breast cancer cells. Cancer Res 2005;65:11118–28.
15. Motoyama AB, Hynes NE, Lane HA. The efficacy of ErbB receptor-targeted anticancer therapeutics is influenced by the availability of epidermal growth factor-related peptides. Cancer Res 2002;62:3151–8.
16. Ritter CA, Perez-Torres M, Rinehart C, et al. Human breast cancer cells selected for resistance to trastuzumab *in vivo* overexpress epidermal growth factor receptor and ErbB ligands and remain dependent on the ErbB receptor network. Clin Cancer Res 2007;13:4909–19.
17. Anido J, Scaltriti M, Bech Serra JJ, et al. Biosynthesis of tumorigenic HER2 C-terminal fragments by alternative initiation of translation. EMBO J 2006;25:3234–44.
18. Saez R, Molina MA, Ramsey EE, et al. p95HER-2 predicts worse outcome in patients with HER-2-positive breast cancer. Clin Cancer Res 2006;12:424–31.
19. Polakis P. Arming antibodies for cancer therapy. Curr Opin Pharmacol 2005;5:382–7.
20. Lambert JM. Drug-conjugated monoclonal antibodies for the treatment of cancer. Curr Opin Pharmacol 2005;5:543–9.
21. Payne G. Progress in immunoconjugate cancer therapeutics. Cancer Cell 2003;3:207–12.
22. Wu AM, Senter PD. Arming antibodies: prospects and challenges for immunoconjugates. Nat Biotechnol 2005;23:1137–46.
23. Bross PF, Beitz J, Chen G, et al. Approval summary: gemtuzumab ozogamicin in relapsed acute myeloid leukemia. Clin Cancer Res 2001;7:1490–6.
24. Chari RV, Martell BA, Gross JL, et al. Immunoconjugates containing novel maytansinoids: promising anticancer drugs. Cancer Res 1992;52:127–31.
25. Remillard S, Rebhun LI, Howie GA, Kupchan SM. Antimitotic activity of the potent tumor inhibitor maytansine. Science 1975;189:1002–5.
26. Helft PR, Schilsky RL, Hoke FJ, et al. A phase I study of cantuzumab mertansine administered as a single intravenous infusion once weekly in patients with advanced solid tumors. Clin Cancer Res 2004;10:4363–8.
27. Tijink BM, Buter J, de Bree R, et al. A phase I dose escalation study with anti-CD44v6 bivatuzumab mertansine in patients with incurable squamous cell carcinoma of the head and neck or esophagus. Clin Cancer Res 2006;12:6064–72.
28. Tolcher AW, Ochoa L, Hammond LA, et al. Cantuzumab mertansine, a maytansinoid immunoconjugate directed to the CanAg antigen: a phase I, pharmacokinetic, and biologic correlative study. J Clin Oncol 2003;21:211–22.
29. Baselga J, Norton L, Albanell J, Kim Y-M, Mendelsohn J. Recombinant humanized anti-HER2 antibody (Herceptin™) enhances the antitumor activity of paclitaxel and doxorubicin against HER2/neu overexpressing human breast cancer xenografts. Cancer Res 1998;58:2825–31.
30. Pegram M, Hsu S, Lewis G, et al. Inhibitory effects of combinations of HER-2/neu antibody and chemotherapeutic agents used for treatment of human breast cancers. Oncogene 1999;18:2241–51.
31. Konecny GE, Thomssen C, Lück HJ, et al. HER-2/neu gene amplificaton and response to paclitaxel in patients with metastatic breast cancer. J Natl Cancer Inst 2004;96:1141–51.
32. Burstein HJ, Keshaviah A, Baron AD, et al. Trastuzumab plus vinorelbine or taxane chemotherapy for HER2-overexpressing metastatic breast cancer: the trastuzumab and vinorelbine or taxane study. Cancer 2007;110:965–72.
33. Kurebayashi J, Otsuki T, Tang CK, et al. Isolation and characterization of a new human breast cancer cell line, KPL-4, expressing the Erb B family receptors and interleukin-6. Br J Cancer 1999;79:707–17.
34. Kovtun YV, Audette CA, Ye Y, et al. Antibody-drug conjugates designed to eradicate tumors with homogeneous and heterogeneous expression of the target antigen. Cancer Res 2006;66:3214–21.
35. Finkle D, Quan ZR, Asghari V, et al. HER2-targeted therapy reduces incidence and progression of midlife mammary tumors in female murine mammary tumor virus huHER2-transgenic mice. Clin Cancer Res 2004;10:2499–511.
36. Austin CD, Wen X, Gazzard L, Nelson C, Scheller RH, Scales SJ. Oxidizing potential of endosomes and lysosomes limits intracellular cleavage of disulfide-based antibody-drug conjugates. Proc Natl Acad Sci U S A 2005;102:17987–92.
37. Lewis GD, Figari I, Fendly B, et al. Differential responses of human tumor cell lines to anti-p185HER2 monoclonal antibodies. Cancer Immunol Immunother 1993;37:255–63.
38. Vogel CL, Cobleigh MA, Tripathy D, et al. Efficacy and safety of trastuzumab as a single agent in first-line treatment of HER2-overexpressing metastatic breast cancer. J Clin Oncol 2002;20:719–26.
39. Cobleigh MA, Vogel CL, Tripathy D, et al. Multinational study of the efficacy and safety of humanized anti-HER2 monoclonal antibody in women who have HER2-overexpressing metastatic breast cancer that has progressed after chemotherapy for metastatic disease. J Clin Oncol 1999;17:2639–48.
40. Romond EH, Perez EA, Bryant J, et al. Trastuzumab plus adjuvant chemotherapy for operable HER2-positive breast cancer. N Engl J Med 2005;353:1673–84.
41. Piccart-Gebhart MJ, Procter M, Leyland-Jones B, et al. Trastuzumab after adjuvant chemotherapy in HER2-positive breast cancer. N Engl J Med 2005;353:1659–72.
42. Geyer CE, Forster J, Lindquist D, et al. Lapatinib plus capecitabine for HER2-positive advanced breast cancer. N Engl J Med 2006;355:2733–43.
43. Erickson HK, Park PU, Widdison WC, et al. Antibody-maytansinoid conjugates are activated in targeted cancer cells by lysosomal degradation and linker-dependent intracellular processing. Cancer Res 2006;66:4426–33.
44. Xie H, Audette C, Hoffee M, Lambert JM, Blättler WA. Pharmacokinetics and biodistribution of the antitumor immunoconjugate, cantuzumab mertansine (huC242-1), and its two components in mice. J Pharmacol Exp Ther 2004;308:1073–82.
45. Austin CD, De Maziere AM, Pisacane PI, et al. Endocytosis and sorting of ErbB2 and the site of action of cancer therapeutics trastuzumab and geldanamycin. Mol Biol Cell 2004;15:5268–82.